UC San Diego

UC San Diego Previously Published Works

Title

Imaging of Cell Morphology Changes via Metamaterial-Assisted Photobleaching Microscopy

Permalink

https://escholarship.org/uc/item/3pc9t8b1

Journal

Nano Letters, 21(4)

ISSN

1530-6984

Authors

Lee, Yeon Ui
Posner, Clara
Zhao, Junxiang
et al.

Publication Date

2021-02-24

DOI

10.1021/acs.nanolett.0c04529

Peer reviewed

eScholarship.org Powered by the California Digital Library
University of California

Author Manuscript

Author Manuscript

Author Manuscript

Author Manuscript

HHS Public Access

Author manuscript

Nano Lett. Author manuscript; available in PMC 2022 February 19.

Published in final edited form as:

Nano Lett. 2021 February 24; 21(4): 1716–1721. doi:10.1021/acs.nanolett.0c04529.

Imaging of cell morphology changes via metamaterial-assisted photobleaching microscopy

Yeon Ui Lee[1], **Clara Posner**[2], **Junxiang Zhao**[1], **Jin Zhang**[2], **Zhaowei Liu**[1,3,*]

[1]Department of Electrical and Computer Engineering, University of California, San Diego, 9500 Gilman Drive, La Jolla, California 92093, United States

[2]Department of Pharmacology, University of California, San Diego, 9500 Gilman Drive, La Jolla, California 92093, United States

[3]Materials Science and Engineering, University of California, San Diego, 9500 Gilman Drive, La Jolla, California 92093, United States

Abstract

Determining the axial position of an emitter with nanoscale precision is critical to a fundamental imaging methodology. While there are many advanced optical techniques being applied to high-resolution imaging, high-axial-resolution topography imaging of living cells is particularly challenging. Here, we present an application of metamaterial-assisted photobleaching microscopy (MAPM) with high-axial resolution to characterize morphological properties of living cells. Quantitative imaging of changes in the morphology of live cells is obtained by topographic and statistical analysis. The time-lapse topography image using the metamaterial-induced photostability provides information about growth factor induced changes in cell morphology with high-axial-resolution.

Graphical Abstract

[*]**Corresponding Author Zhaowei Liu** − *Department of Electrical and Computer Engineering, University of California, San Diego, 9500 Gilman Drive, La Jolla, California 92093, USA; Material Science and Engineering Program, University of California, San Diego, 9500 Gilman Drive, La Jolla, California 92093, USA*; zhaowei@ucsd.edu.

Author Contributions

Y.U.L. and Z.L. conceived and designed the experiment. Y.U.L. and J.Z. performed the experiments. C.P. prepared biological samples. Y.U.L. developed the algorithm and wrote the codes for image processing. Y.U.L. wrote the manuscript which was revised by all authors.

ASSOCIATED CONTENT

Supporting Information.

The Supporting Information is available free of charge at http://pubs.acs.org/

SI 1. Metamaterial-assisted photobleaching microscopy

SI 2. Super-axial-resolution image of the Cos-7 cells

SI 3. Time-lapse MAPM imaging of a HeLa cell after EGF treatment

Author Manuscript Author Manuscript Author Manuscript Author Manuscript

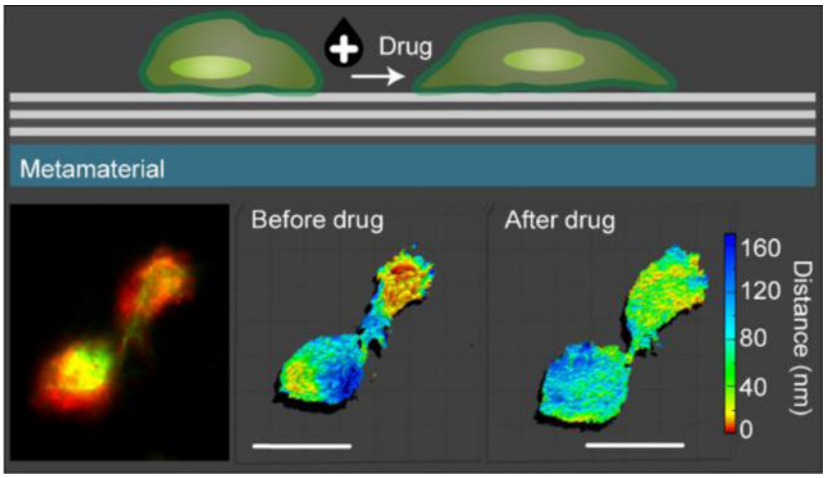

Keywords

Metamaterials; Hyperbolic metamaterials; Super-axial-resolution microscopy; Topographic imaging; Morphology changes; Photobleaching

In the last two decades, fluorescence microscopy is widely used to optically image and analyze biological specimens. Although imaging techniques such as 4Pi-reversible fluorescent saturable optical transition (RESOLFT),[1] interferometric photoactivation and localization microscopy (iPALM),[2] and stochastic optical reconstruction microscopy (STORM)[3] provide three-dimensional super-resolution imaging of biological cell structure, these optical imaging methods meet technical difficulties to achieve axial resolutions below 10 nm. In addition, complicated optical systems are also required in order to obtain a topographic imaging of cell morphology.[4] Monitoring of dynamic changes in the cell morphology is certainly useful for a better understanding of its dynamic processes. We believe that in order to obtain accurate statistical analysis of the cell morphology, it is necessary to acquire information on local distance associated with cell movement through the measurement of time-lapse topography images.

A combination of the super-resolution imaging techniques and plasmonics can fundamentally increase the capabilities of fluorescence microscopy. Recently, we have developed an imaging technique, metamaterial assisted photobleaching microscopy (MAPM), to determine the axial position of fluorophores above a substrate surface with nanometer accuracy (~2.4 nm).[5] Photobleaching lifetime of fluorophores is lengthened when brought into the vicinity of the metamaterial surface. The photobleaching lifetime modification of dipole emitters is well described by the distance-dependent Purcell effect.[6–11] Therefore, metamaterial-induced photobleaching lifetime modification can be used to axially localize the position of the fluorophore above the metamaterial with nanometer accuracy. MAPM using photobleaching lifetime measurement does not require any additional optical modules. Since every pixel acquires an emission signal at the same time with a reasonable imaging speed, it is adaptable for the analysis of cell morphology changes with nanometer accuracy.

Author Manuscript Author Manuscript Author Manuscript Author Manuscript

In this study, we present MAPM imaging applications for analyzing the epidermal growth factor (EGF)-induced cell morphology changes in live cells (Figure 1a, b). Extended MAPM technique to analyze image stacks from time-lapse sequences allow functionalized imaging of dynamic morphology changes of live cells. Figure 1c, d show the simplified representation of fluorescent protein as a dipole emitter within a cell membrane situated close to a planar hyperbolic metamaterial (HMM) substrate with separation distance *d*. The correlation between photobleaching lifetime and distance above the HMM surface is given by the distance-dependent Purcell effect (Figure S1).[5] The planar HMM provides enhanced Purcell effect over a broadband spectral range[12,13], which is essential for multicolor MAPM imaging technology. The time-lapse topography image using the metamaterial-induced photostability provides information about cell morphology changes with super-axial-resolution.

Cos-7 cells were grown on top of the HMM substrate and then transiently transfected (see Method section 'Cell transfection' for details.). Cell samples with fluorescently labeled actin (Lifeact-Venus) situated on the HMM substrate were excited by a CW laser of wavelength 488 nm at the laser intensity of about 23 W/cm^2. The fluorescence intensity images were collected by an objective lens (40× / 0.6 NA) and a magnification tube lens (2×) and then detected by a sCMOS camera with an emission filter (520/40 nm) (see Methods and Figure S1 for details.). In the experiment, a stack of fluorescence microscopy images consisting of 500 frames was collected in 200 seconds (2.5 frames per second; 2.5 fps). An averaged fluorescence image of a Cos-7 cell is shown in Figure 2a. Figure 2b shows the photobleaching-lifetime image with a strong spatial dependence. The distance from the HMM surface to the fluorescent protein can be obtained for each pixel according to the pre-calculated and pre-measured axial distance-dependence of the photobleaching lifetime, and the resulting MAPM images are shown in Figure 2c, d. The distance image of the fluorescently labeled actin shows the spatial variation of the distance in the range of 2–160 nm. Additional morphological images of Cos-7 cells are shown in Figure S2. Reproducibility of our MAPM technique was tested by repeating the MAPM imaging procedures with over 20 different Cos-7 cells. The spatial distribution of distance between cell and the HMM surface could result from the spatial difference in cellular structures or the heterogeneity of the cell.[5,14]

Having discussed the basic principle, we now test the capability of MAPM to observe the influence of the drug treatment on cell morphology. It is well known that the epidermal growth factor (EGF) stimulates differentiation, migration, cell growth, and cell adhesion changes[15,16] by binding to its receptor. HeLa cells were grown on top of the HMM substrate and then transiently transfected with a fluorescent protein targeted to the plasma membrane using the C-terminal CAAX sequence of KRas (Venus-CAAX) (see Method section 'Cell transfection' for details). The fluorescence intensity image sequences of 500 frames of HeLa cells were collected in 200 seconds (2.5 frames per second; 2.5 fps), while the fluorophores are excited with a constant laser intensity of about 23 W/cm^2 for the wide field of view. An averaged fluorescence images of HeLa cells are shown in Figure 3a. After 15 minutes of incubation with epidermal growth factor (EGF, 10 ng/ml), another 500 frames of images of the growth-factor treated cells were collected. An averaged fluorescence intensity image of the EGF-treated HeLa cells is shown in Figure 3b with the merged image (Figure 3c). The

Author Manuscript Author Manuscript Author Manuscript Author Manuscript

same exposure time, pH of buffer solutions and the temperature of the chamber were used during the data collection period for each measurement data set. Cells showed negligible movement during a short photobleaching measurement cycle (500 frames, 200 seconds).

In the post-reconstruction processing of the collected data, the photobleaching signals were fitted for each pixel, and the photobleaching lifetimes were extracted (Figure 3d, f). In addition to information on the modification of the size and shape of growth factor treated HeLa cells in the intensity images, the photobleaching-lifetime images show additional information about spatial heterogeneity. By measuring photobleaching lifetime, positions of the plasma membrane localized proteins are obtained with nanometer axial precision. From the MAPM reconstructed images (Figure 3e, g) showing the distances between the fluorescence proteins to the HMM surface with a super-axial resolution, one can easily observe that the cells spread out after the drug treatment. Treatment with EGF significantly changes cell morphology. Arrows denote cell pre-settled/floating/spreading over the HMM substrate. Additional representative images and analysis of the changes in cell morphology are provided in Figure 4.

Imaging of the time-lapse series was performed to observe EGF stimulated cell morphology changes over a longer time span after drug treatment. 500 frames were collected every 400 ms over a period of 200 seconds, in which sufficient distance-dependent photobleaching signals were acquired for each pixel. Cell movement during each imaging cycle was minimal. Averaged fluorescence intensity images of the HeLa cell stimulated with EGF after the indicated time are shown in Figure 5a, b with the merged image (Figure 5c). Interestingly, MAPM reconstructed images (Figure 5d, e, f) show significant information about cell morphology that does not appear in the intensity images. Direct quantification is presented in the MAPM reconstructed images, showing the cell protrusion and retraction. The observed cell morphology changes in the three snapshots describe the formation of individual cell-substrate contacts, i.e., domains which are located in the vicinity of the top surface of the substrate, with nanometer accuracy. Additional representative images are shown in Figure S3.

In conclusion, we demonstrated MAPM imaging applications for analyzing the epidermal growth factor (EGF)-induced morphology changes in live cells with super-axial-resolution. We experimentally developed an extended MAPM imaging technique to analyze image stacks from time-lapse sequences for the combined time-lapse and topographic imaging, and in particular of cellular systems, based on the use of MAPM. For the purpose of obtaining precise distance information with axial resolution below 10 nm between cell and substrate, MAPM could be one of the simplest and most user friendly imaging methods. We believe MAPM is a useful imaging method for live cell morphology studies, and future studies will combine this method with strategies for lateral resolution improvement.

Methods

Experimental set-up

A custom-modified fluorescence microscopy, Olympus IX83 with upright configuration was utilized. A 488 nm laser coupled through a multimode fiber was used to excite fluorescently

Author Manuscript Author Manuscript Author Manuscript Author Manuscript

labeled biological samples and 500 frames of fluorescence signal were collected by an objective lens (0.6 NA) and an sCMOS camera with proper color filters. A 488 dichroic mirror and a 520/40 nm band-pass filter were adopted. The reduction in emission intensity over time of the acquired fluorescence signal was mathematically fitted and analyzed for each pixel using MATLAB. We use MATLAB to adjust data acquisition card (DAQ) voltage output module to synchronize laser beam shutters and acquisition modules properly. All cells were kept in a humidified incubator at 37°C with a 5% CO_2 atmosphere during time-lapse MAPM imaging.

Cell transfection

Cells were cultured in Dulbecco modified Eagle medium (DMEM; Gibco) containing 4.5 g/L glucose and supplemented with 10% (v/v) fetal bovine serum (FBS, Sigma) and 1% (v/v) penicillin-streptomycin (Pen-Strep, Sigma-Aldrich). All cells were maintained in a humidified incubator at 37°C with a 5% CO_2 atmosphere. 24 hours prior to transfection, cells were seeded onto HMM substrate and grown to 50–70% confluence. **Cos-7 cell transfection.** Cos7 cells were then transfected with 100 ng of pcDNA3-Lifeact-Venus using Lipofectamine 2000 (Invitrogen) and grown an additional 24 h before fixation. Cells were washed with Phosphate-buffered saline (PBS) before fixation with 4% paraformaldehyde and 0.2% glutaraldehyde PBS for 10 min at room temperature. Cells were quickly rinsed in PBS after fixation and quenched with freshly made 0.1% NaBH4 ice-cold PBS. After quenching, cells were washed three times for five minutes each with PBS on a shaker. Cells were imaged at room temperature. **HeLa cell transfection.** HeLa cells were then transfected with 100 ng of pcDNA3-Venus-CAAX (87612, Addgene) for plasma membrane labeling using Lipofectamine 2000 (Invitrogen) and grown an additional 24 h. Cells were imaged at room temperature.

Supplementary Material

Refer to Web version on PubMed Central for supplementary material.

ACKNOWLEDGMENT

This work was supported by the Gordon and Betty Moore Foundation (to Z. Liu) and NIH R35 CA197622 (to J. Zhang). C. Posner was supported by the Molecular Biophysics Training Grant, NIH Grant T32 GM008326. The authors thank Q. Ma and G. Li for sample preparation.

REFERENCES

(1). Böhm U; Hell SW; Schmidt R. 4Pi-RESOLFT Nanoscopy. Nat. Commun. 2016, 7 (1), 10504. 10.1038/ncomms10504. [PubMed: 26833381]

(2). Shtengel G; Galbraith JA; Galbraith CG; Lippincott-Schwartz J; Gillette JM; Manley S; Sougrat R; Waterman CM; Kanchanawong P; Davidson MW; et al. Interferometric Fluorescent Super-Resolution Microscopy Resolves 3D Cellular Ultrastructure. Proc. Natl. Acad. Sci. 2009, 106 (9), 3125–3130. 10.1073/pnas.0813131106. [PubMed: 19202073]

(3). Xu K; Babcock HP; Zhuang X. Dual-Objective STORM Reveals Three-Dimensional Filament Organization in the Actin Cytoskeleton. Nat. Methods 2012, 9 (2), 185–188. 10.1038/nmeth.1841. [PubMed: 22231642]

Author Manuscript Author Manuscript Author Manuscript Author Manuscript

(4). Kanchanawong P; Shtengel G; Pasapera AM; Ramko EB; Davidson MW; Hess HF; Waterman CM Nanoscale Architecture of Integrin-Based Cell Adhesions. Nature 2010, 468 (7323), 580–584. 10.1038/nature09621. [PubMed: 21107430]

(5). Lee YU; Zhao J; Mo GCH; Li S; Li G; Ma Q; Yang Q; Lal R; Zhang J; Liu Z. Metamaterial-Assisted Photobleaching Microscopy with Nanometer Scale Axial Resolution. Nano Lett. 2020, 20 (8), 6038–6044. 10.1021/acs.nanolett.0c02056. [PubMed: 32597659]

(6). Vasilev K; Stefani FD; Jacobsen V; Knoll W; Kreiter M. Reduced Photobleaching of Chromophores Close to a Metal Surface. J. Chem. Phys. 2004, 120 (14), 6701–6704. 10.1063/1.1665719. [PubMed: 15267562]

(7). Muthu P; Gryczynski I; Gryczynski Z; Talent J; Akopova I; Jain K; Borejdo J. Decreasing Photobleaching by Silver Island Films: Application to Muscle. Anal. Biochem. 2007, 366 (2), 228–236. 10.1016/j.ab.2007.04.014. [PubMed: 17531183]

(8). Kéna-Cohen S; Wiener A; Sivan Y; Stavrinou PN; Bradley DDC; Horsfield A; Maier SA Plasmonic Sinks for the Selective Removal of Long-Lived States. ACS Nano 2011, 5 (12), 9958–9965. 10.1021/nn203754v. [PubMed: 22032601]

(9). Zaiba S; Lerouge F; Gabudean A-M; Focsan M; Lermé J; Gallavardin T; Maury O; Andraud C; Parola S; Baldeck PL Transparent Plasmonic Nanocontainers Protect Organic Fluorophores against Photobleaching. Nano Lett. 2011, 11 (5), 2043–2047. 10.1021/nl2004847. [PubMed: 21488657]

(10). Cang H; Liu Y; Wang Y; Yin X; Zhang X. Giant Suppression of Photobleaching for Single Molecule Detection via the Purcell Effect. Nano Lett. 2013, 13 (12), 5949–5953. 10.1021/nl403047m. [PubMed: 24245957]

(11). Lee YU; Wisna GBM; Hsu S; Zhao J; Lei M; Li S; Tao AR; Liu Z. Imaging of Nanoscale Light Confinement in Plasmonic Nanoantennas by Brownian Optical Microscopy. ACS Nano 2020, 14 (6), 7666–7672. 10.1021/acsnano.0c04019. [PubMed: 32438800]

(12). Jacob Z; Smolyaninov II; Narimanov EE Broadband Purcell Effect: Radiative Decay Engineering with Metamaterials. Appl. Phys. Lett. 2012, 100 (18), 181105. 10.1063/1.4710548.

(13). Noginov MA; Li H; Barnakov YA; Dryden D; Nataraj G; Zhu G; Bonner CE; Mayy M; Jacob Z; Narimanov EE Controlling Spontaneous Emission with Metamaterials. Opt. Lett. 2010, 35 (11), 1863. 10.1364/OL.35.001863. [PubMed: 20517443]

(14). Bourg N; Mayet C; Dupuis G; Barroca T; Bon P; Lécart S; Fort E; Lévêque-Fort S. Direct Optical Nanoscopy with Axially Localized Detection. Nat. Photonics 2015, 9 (9), 587–593. 10.1038/nphoton.2015.132.

(15). Kim H-D; Guo TW; Wu AP; Wells A; Gertler FB; Lauffenburger DA Epidermal Growth Factor–Induced Enhancement of Glioblastoma Cell Migration in 3D Arises from an Intrinsic Increase in Speed But an Extrinsic Matrix- and Proteolysis-Dependent Increase in Persistence. Mol. Biol. Cell 2008, 19 (10), 4249–4259. 10.1091/mbc.e08-05-0501. [PubMed: 18632979]

(16). Kedmi M; Ben-Chetrit N; Körner C; Mancini M; Ben-Moshe NB; Lauriola M; Lavi S; Biagioni F; Carvalho S; Cohen-Dvashi H; et al. EGF Induces MicroRNAs That Target Suppressors of Cell Migration: MiR-15b Targets MTSS1 in Breast Cancer. Sci. Signal. 2015, 8 (368), ra29–ra29. 10.1126/scisignal.2005866.

Author Manuscript Author Manuscript Author Manuscript Author Manuscript

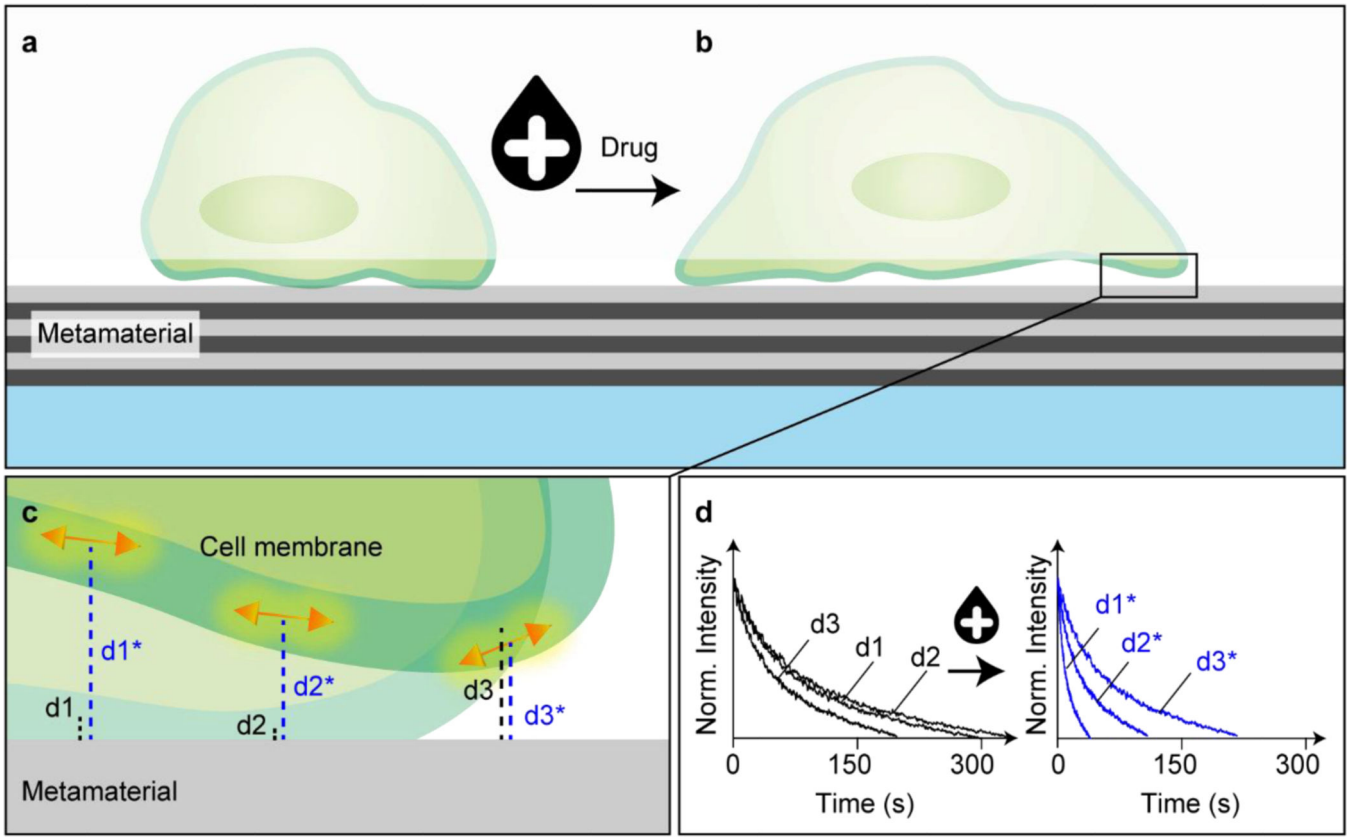

Figure 1. Metamaterial assisted photobleaching microscopy (MAPM) imaging method of EGF-stimulated changes in cancer cell adhesion.

(**a, b**) Treatment of cells with EGF causes cell morphology changes. (**c, d**) Schematics showing the metamaterial assisted photobleaching microscopy (MAPM) configuration. Photobleaching lifetime of fluorophores near the metamaterial is lengthened due to the strong near-field coupling. The bleaching of the fluorescent signal over time provides positions of fluorescent molecules above an HMM surface.

Author Manuscript Author Manuscript Author Manuscript Author Manuscript

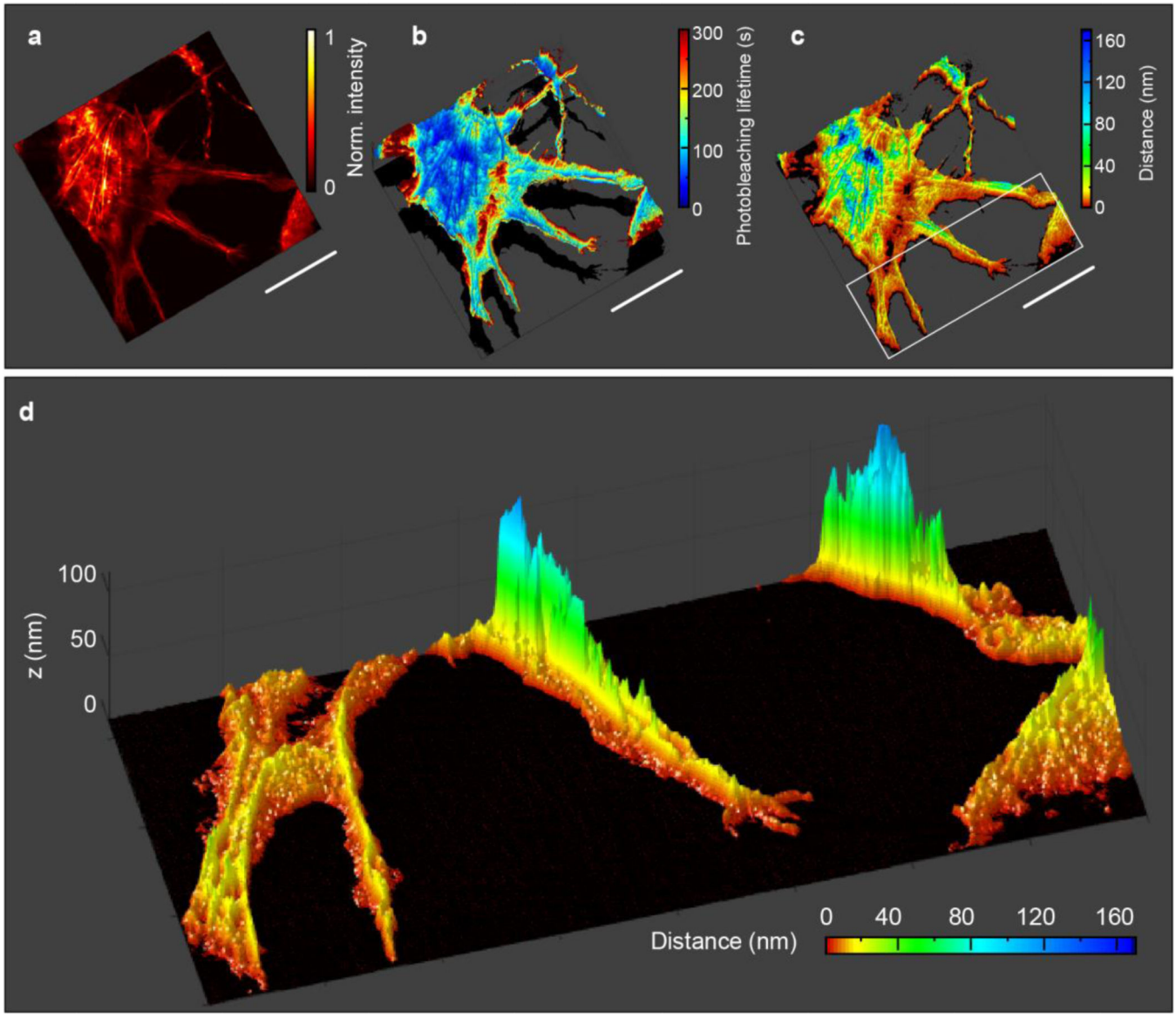

Figure 2. Conventional fluorescence images and MAPM reconstructed super-resolution images of Cos-7 cells.

(**a**) Averaged fluorescence image of fixed Cos-7 cell. A stack of fluorescence microscopy images (500 frames) is converted into a (**b**) photobleaching-lifetime mapping image. (**c**) MAPM reconstructed super axial-resolution image of the Cos-7 cell situated on the HMM substrate. Scale bar: 20 μm. (**d**) Zoom of boxed region in (c).

Author Manuscript Author Manuscript Author Manuscript Author Manuscript

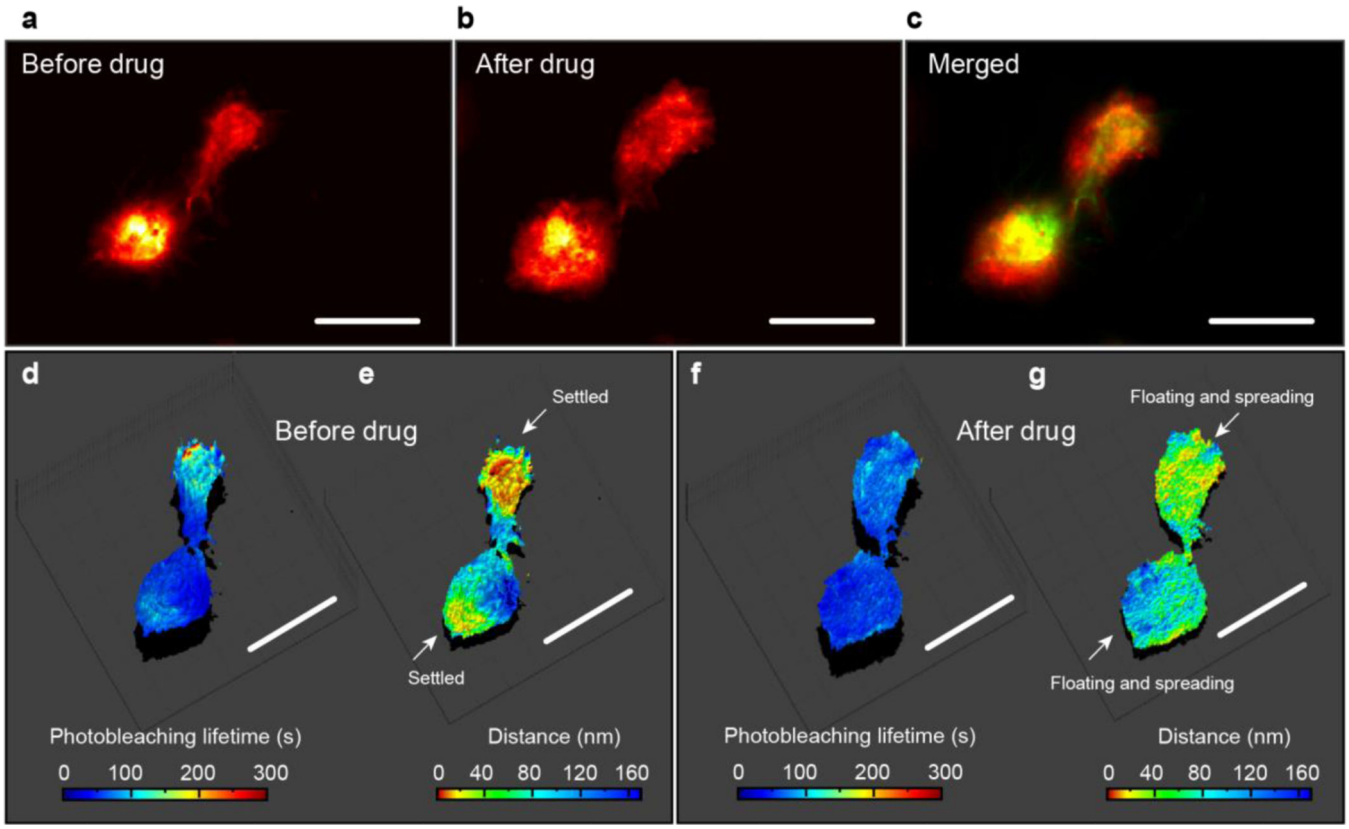

Figure 3. MAPM imaging of EGF-induced morphology changes of HeLa cells.

Averaged intensity images of fluorescently labelled HeLa cell membrane (**a**) before and (**b**) 15 minutes after EGF treatment. (**c**) The merged image. Photobleaching lifetime image and MAPM topography image of the Hela cell which shows the cell morphology changes with nanometer accuracy (**d, e**) before and (**f, g**) after EGF treatment, respectively. Scale bar is 20 μm.

Author Manuscript Author Manuscript Author Manuscript Author Manuscript

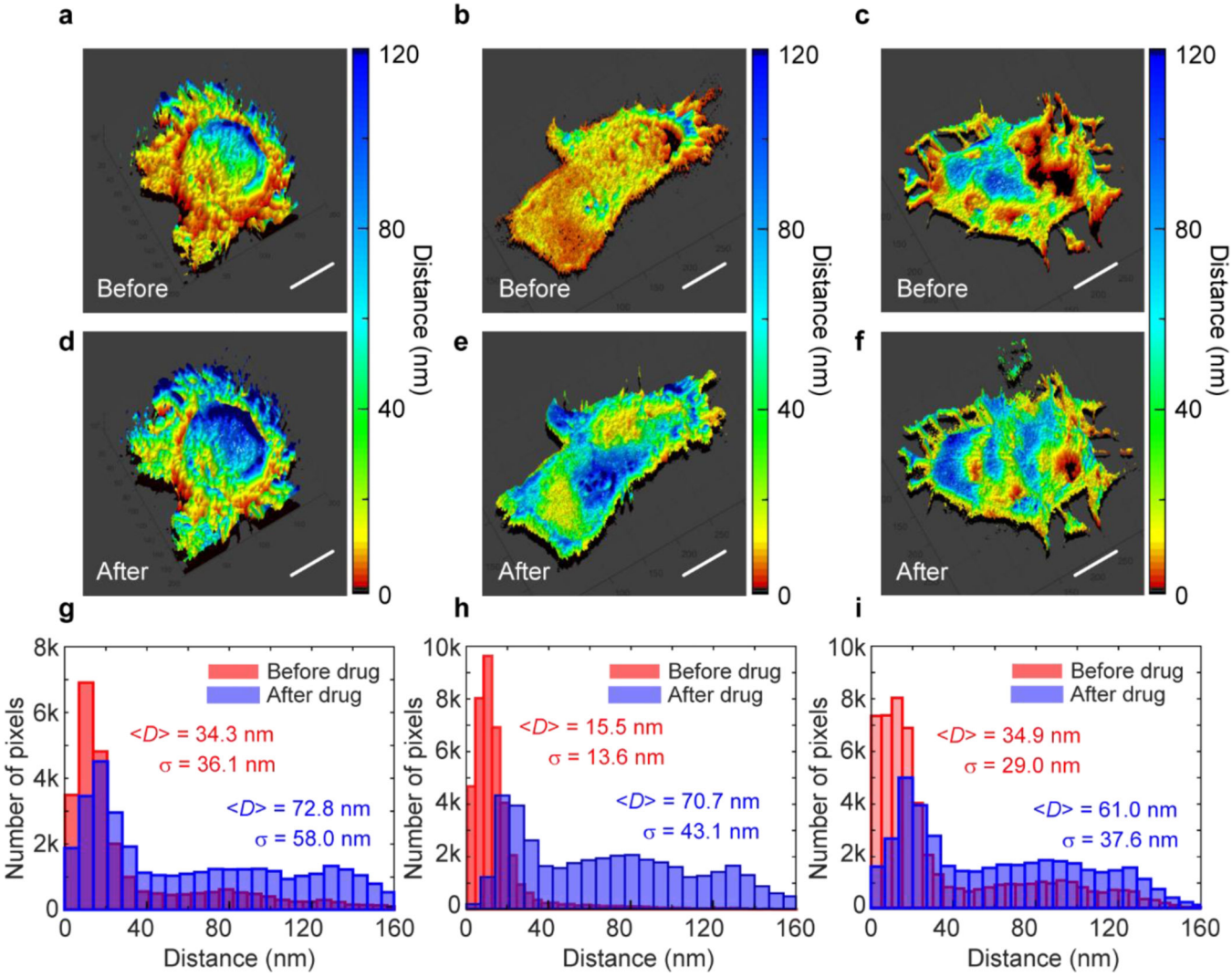

Figure 4. Histograms of the MAPM imaging of EGF-induced morphology changes of HeLa cells.

MAPM reconstructed super-resolution topography images of the Hela cells which show the significant changes in the distance between the cell membrane and the HMM surface (**a-c**) before and (**d-f**) 15 minutes after EGF treatment, respectively. Scale bar is 10 μm. (**g-i**) The statistical distance distributions. The red and blue colored histograms are created from the images for the before and after drug treatment, respectively, yielding averaged distance of $<D>$ and standard deviations of σ.

Author Manuscript Author Manuscript Author Manuscript Author Manuscript

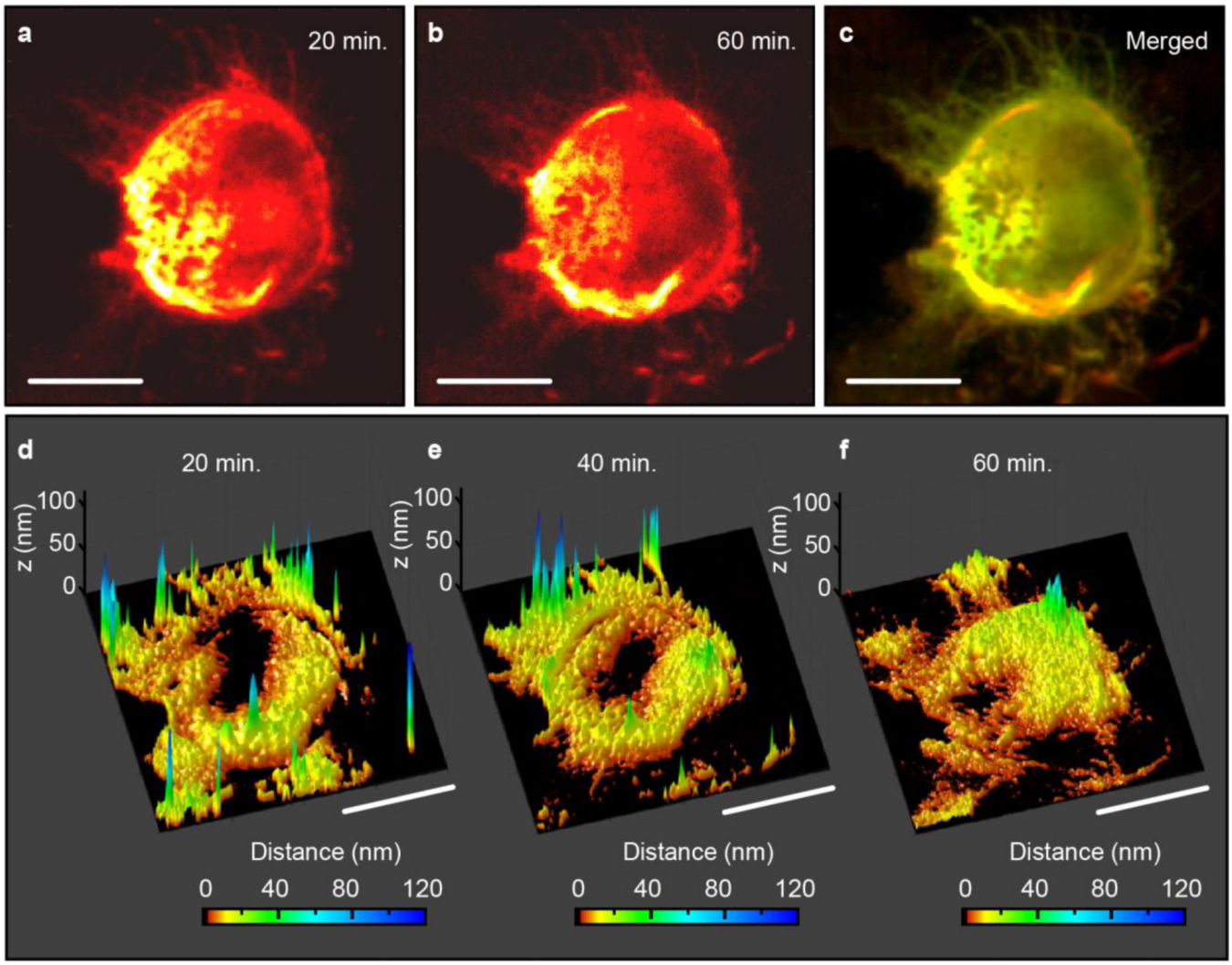

Figure 5. Time-lapse MAPM imaging of a HeLa cell after EGF treatment.

(**a, b**) Averaged fluorescence intensity images of the fluorescently labeled HeLa cell membrane stimulated with EGF, in which the HeLa cell was incubated with EGF for the indicated time. (**c**) The merged image. (**d, e, f**) Time-lapse sequence of MAPM reconstructed images of the Hela cell showing dynamic changes in morphology over a longer time span after drug treatment. The HeLa cell was incubated with EGF for the indicated time. Scale bar is 10 μm.